THE JOURNAL OF BIOLOGICAL CHEMISTRY Vol. 278, No. 36, Issue of September 5, pp. 34181–34188, 2003

Printed in U.S.A.

CRIM1 Regulates the Rate of Processing and Delivery of Bone Morphogenetic Proteins to the Cell Surface*

Received for publication, February 5, 2003, and in revised form, June 10, 2003
Published, JBC Papers in Press, June 12, 2003, DOI 10.1074/jbc.M301247200

Lorine Wilkinson‡, Gabriel Kolle‡§¶, Daying Wen‡, Michael Piper‡, Julie Scott‡, and Melissa Little‡‖

From the ‡Institute for Molecular Bioscience and the §Department of Biochemistry, The University of Queensland, Brisbane, Queensland 4072, Australia

The *Crim1* gene is predicted to encode a transmembrane protein containing six von Willebrand-like cysteine-rich repeats (CRRs) similar to those in the BMP-binding antagonist Chordin (*Chrd*). In this study, we verify that CRIM1 is a glycosylated, Type I transmembrane protein and demonstrate that the extracellular CRR-containing domain can also be secreted, presumably via processing at the membrane. We have previously demonstrated *Crim1* expression at sites consistent with an interaction with bone morphogenetic proteins (BMPs). Here we show that CRIM1 can interact with both BMP4 and BMP7 via the CRR-containing portion of the protein and in so doing acts as an antagonist in three ways. CRIM1 binding of BMP4 and -7 occurs when these proteins are co-expressed within the Golgi compartment of the cell and leads to (i) a reduction in the production and processing of preprotein to mature BMP, (ii) tethering of pre-BMP to the cell surface, and (iii) an effective reduction in the secretion of mature BMP. Functional antagonism was verified by examining the effect of co-expression of CRIM1 and BMP4 on metanephric explant culture. The presence of CRIM1 reduced the effective BMP4 concentration of the media, thereby acting as a BMP4 antagonist. Hence, CRIM1 modulates BMP activity by affecting its processing and delivery to the cell surface.

The TGFβ[1] superfamily of ligands have prominent roles in nearly all tissues during development. There are over 30 members of this superfamily, including the TGFβ isoforms, bone morphogenetic proteins (BMPs), and the closely related growth and differentiation factors, activins, and nodals (reviewed in Ref. 1). BMPs, like all members of the TGFβ superfamily, are synthesized as preproteins, which are subsequently cleaved by furin and related subtilisin-like convertases within the Golgi apparatus at a conserved multibasic amino acid motif (Arg-*X*-*X*-Arg) to yield a dimeric C-terminal mature domain (2). Once secreted BMPs bind and facilitate the formation of heteromeric complexes of type I and type II serine/threonine kinase receptors (1). These signal via phosphorylation of Smad proteins, which can translocate into the nucleus and effect gene regulation and expression (reviewed in Ref. 1). Although TGFβ-1, -2, and -3 are secreted as a member of a large inactive complex containing the latency-associated peptide and a latent TGFβ-binding protein, the BMPs are currently thought to be processed and secreted as active mature molecules and not complexed with a latent TGFβ-binding protein-like molecule. However, like the TGFβs, BMPs do not seem to act over a range of more than one to two cells, suggesting that there is some mechanism of "tethering" (3). This limit in signaling range is in part influenced by the prodomain of BMPs (3). The prodomain of the BMPs also influences the efficiency of processing and the stability of the mature BMP (2, 4). During development, TGFβ superfamily members, and in particular BMPs, specify cell types by forming precisely controlled concentration gradients. The amount of active ligand is regulated via modulation of protein processing, receptor binding, regulation of Smad function, and, as has been discovered recently, extracellular antagonism of BMPs. One of the extracellular BMP antagonists is Chordin (*Chrd*) and its homologue in *Drosophila*, short gastrulation (*sog*) (5–8). The Chordin protein (CHRD) is a dorsalizing factor expressed by the organizer in *Xenopus*, which functions by directly binding BMP4 to inhibit its receptor binding (5, 8). *Sog*, the functional homologue of *Chrd* in *Drosophila*, is expressed ventrally and partly establishes the dorso-ventral body axis by inhibiting the activity of *dpp* (most closely related to vertebrate BMP2/4) (6). Overexpression of SOG protein can inhibit BMP4 signaling in *Xenopus*, revealing functional conservation of this interaction between vertebrates and invertebrates (7). The BMP-antagonizing activity of CHRD and SOG is itself regulated via secreted metalloproteases related to BMP1 (9, 10). Xolloid in *Xenopus* cleaves CHRD, effectively abolishing its ability to antagonize BMP4 (9). Tolloid functions in a similar way in *Drosophila* to cleave SOG (10).

CHRD and SOG proteins are characterized by multiple cysteine-rich repeats, similar to the von Willebrand Factor type C domain (5). Such cysteine-rich repeats (CRRs) have a conserved consensus sequence based on ten cysteines ($CX\text{n}WX_4CX_2CXCX_6CX_4CX_{4-6}CX_{9-11}CCPXC$). Specific individual CRRs in CHRD can bind directly to BMP4 (11). Recently, a number of novel CRR-containing proteins have been identified, including Neuralin1 (also known as Ventropin) (12–14), *Drosophila* Crossveinless*2* (15), and *Xenopus* Kielen (16). Although possessing varying numbers of CRRs, all of these proteins bind to BMPs. CRR motifs in other proteins mediate binding to other members of the TGFβ superfamily. The CRR of

* This work was supported in part by the National Health and Medical Research Council (NMHRC) of Australia (Grant 102578) and the Sylvia and Charles Viertel Charitable Trust. The costs of publication of this article were defrayed in part by the payment of page charges. This article must therefore be hereby marked "*advertisement*" in accordance with 18 U.S.C. Section 1734 solely to indicate this fact.

In memory of our colleague Dr. Toshiya Yamada, 1960–2001.

¶ Holds an Australian Postgraduate Award.

‖ An NHMRC Senior Research Fellow and a Sylvia and Charles Viertel Senior Research Fellow. To whom correspondence should be addressed. Tel.: 61-7-3365-4494 (ext. 1819); Fax: 61-7-3365-4388; E-mail: M.Little@imb.uq.edu.au.

[1] The abbreviations used are: TGFβ, transforming growth factor β; BMP, bone morphogenetic protein; CHRD, chordin; CRR, cysteine-rich repeat; GHR, growth hormone receptor; FGFR, fibroblast growth receptor; DTT, dithiothreitol; PBS, phosphate-buffered saline; HA, hemagglutinin.

procollagen type IIA can interact with TGFβ2 and BMP2 (11, 17). It has therefore been speculated that this domain has evolved to modulate interactions with TGFβ superfamily members (11). Connective tissue growth factor contains one CRR and has been shown to antagonize BMP4 by inhibiting receptor binding but acts synergistically with TGFβ1 to enhance receptor binding (18). Therefore this novel family of proteins appear critical in regulating the activity of TGFβ/BMP signaling in development.

The *Crim1* gene encodes a protein with six chordin-like CRRs, an N-terminal insulin-like growth factor binding protein-like motif and a putative transmembrane domain (19). By analogy to other CRR proteins, we have hypothesized that CRIM1 may also function as an antagonist to one or more members of the TGFβ superfamily by direct binding via the CRR repeats (19). *Crim1* shows developmentally regulated expression in the mouse embryo localized to the developing kidney and testis (20), the lens of the eye (21), vibrissae, pinna, tooth primordia, as well as specific regions within the central nervous system (19). A study of the spatial and temporal expression of *Crim1*, *BMP2*, and *BMP7* during mouse urogenital development, showed a pattern of overlapping expression for these proteins implying a possible physiological interaction (20). Here we show that CRIM1 interacts with members of the TGFβ family, including BMP4 and BMP7, when co-expressed with these growth factors and that this interaction occurs via the CRR repeat domains. Co-expression of CRIM1 with BMP4 or BMP7 results in a reduction in the processing of pre-BMPs to their mature form and a consequent reduction in the amount of BMP secretion. However, CRIM1 is trafficked with its preprotein ligand to the plasma membrane, whereupon a proportion of the complex remains tethered to the cell surface in an inactive preprotein form. Hence CRIM1 can antagonize members of the TGFβ superfamily.

EXPERIMENTAL PROCEDURES

Construction of Mammalian Expression Vectors—A full-length human CRIM1 (GenBank™ accession number AF167706) expression construct was created from existing subclones, which covered the entire open reading frame of CRIM1. Intrinsic *Pme*I and *Dra*II restriction enzyme sites were used for insertion into pCDNA3. An myc (EQKLISEEDL) or HA (YPYDVPDY) tag was introduced into CRIM1-N$^{myc/HA}$ constructs after residue 78 (Phe) by PCR. CRIM1-E was made by truncating the protein at residue 901, and inserting an myc or HA tag at the C terminus. BMP7^{preHA} was derived from mouse BMP-7 (pMTAD1-BMP7^{myc}, a gift of Dr. Elizabeth Robertson) by inserting the HA epitope after residue 87 (Tyr) as a linker in an intrinsic *Bsr*GI site. Other constructs used in this study were human BMP4 (PMT21-BMP4^{myc}, a gift of Dr. Tom Jessell), chicken Chordin (pMT21-CHRD^{HA}, a gift of Dr. Kevin Lee), and human growth hormone receptor (pcDNA3-GHR^{HA} , a gift of Prof. Michael Waters).

Generation of Anti-CRIM1 Antibodies—Polyclonal antibodies were raised and purified as described previously (26). α-NC was raised toward a synthetic peptide: KVCQPGYLNILVSKASGKPGEC (Chiron Technologies). α-CC was raised toward a glutathione *S*-transferase-conjugated C-terminal epitope of mouse CRIM1 (residues 998–1036; GenBank™ accession number AF168680), which was cloned into pGEX as described previously (26).

Cell Culture and Transfections—COS7 cells were transfected when at 50–70% confluence with 1 μg of DNA (or as indicated), in 3 μl of FuGENE6 (Roche Applied Science). Transfected cells were incubated in Dulbecco's modified Eagle's medium plus 10% fetal calf serum or OPTI-MEM (Invitrogen) for serum-free conditions for 2–3 days. Conditioned media was harvested and concentrated 10× using Amicon Ultra concentraters (Millipore).

Cell Fractionation and Western Blotting—CRIM1-N^{myc}-transfected COS7 cells were fractionated into light membrane, heavy membrane, and soluble fractions as previously described (22). Western blotting, of fractionated samples, cellular extracts, or media as described below, was performed as described previously (26).

Immunofluorescence of Cells—Immunofluorescence on cell lines using the antibodies indicated was performed as described previously for permeabilized cells (26). For cell surface binding, antibody incubations were performed on live cells incubated on ice to inhibit internalization. Cells were finally fixed in 4% paraformaldehyde for 30 min. Antibody labeling was captured on an Olympus AX70 compound fluorescence microscope.

Protein Expression and Glycosylation Assay—For production of CRIM1, CHRD, BMP4, or BMP7 for *in vitro* binding studies, transiently transfected COS7 cells were incubated in serum-free OPTI-MEM (Invitrogen) for 2 days. Conditioned media was concentrated 1:10 and snap-frozen. Conditioned media from transfections using pcDNA3 without insert were used as a control. CRIM1-E protein was expressed by using a stable Chinese hamster ovary cell line. The protein was purified from conditioned media on an α-myc affinity column. The α-myc produced by the hybridoma 9E10 was cross-linked to protein A-agarose (Sigma) using the method supplied with the cross-linker (Pierce). Protein concentrations were estimated against samples of known concentration by Western blotting. *N*-Glycosidase S was used to determine *N*-linked glycosylation according to the manufacturer's instructions (Roche Applied Science).

Immunoprecipitation—For *in vitro* binding experiments, conditioned concentrated media (see above) were incubated in 200 μl of 0.5% bovine serum albumin, 5 mM Tris-HCl, pH 8.0, for 3 h on ice. Cross-linking was performed where indicated using disuccinimidyl suberate (Pierce) according to the manufacturer's instructions. For immunoprecipitation of co-expressed samples, media was used without concentration. Immunoprecipitations were performed by the addition of 5 μl of α-myc antibody and a 2-h incubation at room temperature, followed by the addition of 40 μl of protein A-Sepharose (50% slurry, Sigma) and a further 1-h incubation. The beads were pelleted and washed four times with PBS 0.1% Triton X-100 and once with PBS. Protein was eluted by addition of SDS-PAGE loading buffer (0.625 M Tris-HCl, pH 6.8, 4% SDS, 10% β-mercaptoethanol, 40% glycerol, 0.05% bromphenol blue) and boiled for 5 min. For cellular extracts, transfected cells were suspended in 600 μl of lysis buffer (0.05 M Tris, 0.15 M NaCl, pH 8.5, Complete protease inhibitors (Roche Applied Science), 0.5% Triton X-100). Immunoprecipitation was carried out as above, except that beads were pelleted and washed in lysis buffer three times, and twice in PBS.

Biotinylation—Cell surface proteins were biotinylated using EZ-Link Sulfo-NHS-LC-Biotin according to the manufacturer's instructions (Pierce).

Explant Culture—Embryonic mouse kidneys were dissected at 11.5 days postcoitum (dpc) and grown in culture medium containing Dulbecco's modified Eagle's medium/F-12, 20 mM glutamine, 5 μg/ml holo-Transferrin as described in a previous study (27). Conditioned medium (5 μl) was added where indicated. For immunofluorescence analyses, explants were fixed in 100% ice-cold methanol, 10 min, washed in PBS, and permeabilized with 1% Triton X-100 in PBS. Antibody incubations were performed for 1 h at 37 °C in 1% bovine serum albumin in PBS. Primary antibodies used were WT1 (DAKO, 1/100 dilution) and calbindin 28K (Sigma, 1/200 dilution). Secondary antibodies were Cy3-conjugated anti-rabbit IgG and Alexa-conjugated anti-mouse IgG. Ureteric tip and nephron number were counted manually, and statistics were performed using InStat3. Due to variability in the age of explants between litters, one-way analysis of variance could only be performed within a given experiment.

RESULTS

CRIM1 Is a Type I Transmembrane Protein—Sequence analysis of the CRIM1 open reading frame reveals a C-terminal transmembrane domain, suggesting the large N-terminal CRR-containing domain localizes in the extracellular space (19). To test this, we designed mammalian expression constructs of human full-length CRIM1, differentially tagged with myc or HA epitope tags (CRIM1-N$^{myc/HA}$). We also produced myc- and HA-tagged constructs with a deletion of the potential transmembrane domain and C-terminal sequence (CRIM1-E$^{myc/HA}$) (Fig. 1*A*). Polyclonal antibodies were raised in rabbits to epitopes in the N and C termini of CRIM1 (α-NC and α-CC, respectively) (Fig. 1*A*). Western blotting with α-myc, α-NC, and α-CC of cellular extracts of COS7 cells transfected with the CRIM1 constructs identified bands of ~140 kDa for CRIM1-N^{myc} and 120 kDa for CRIM1-E^{myc} (Fig. 1, *B* and *C*). CRIM1-E was detected with the α-NC antibody (Fig. 1*C*), but the α-CC epitope is deleted in this construct. A sequence of LV*X*LP*X*-

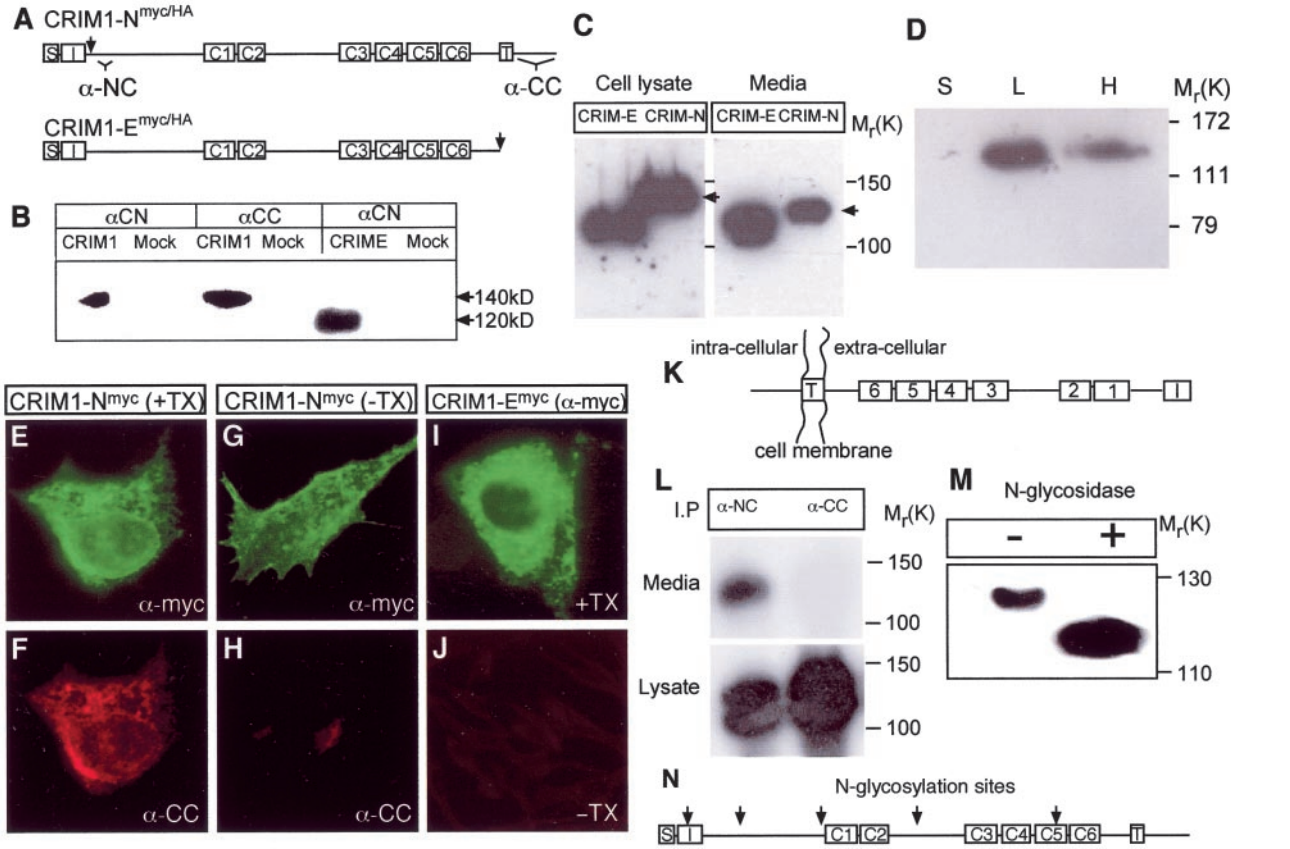

FIG. 1. **CRIM1 is a glycosylated type I transmembrane protein.** *A*, ideogram of CRIM1 expression vectors. Full-length (CRIM1-$N^{myc/HA}$) and C-terminal deleted CRIM1 constructs (CRIM1-$E^{myc/HA}$) were tagged with myc or HA epitopes (*arrows* indicate epitope tag insertions). Regions to which polyclonal antibodies α-NC and α-CC were raised are indicated. *B*, the polyclonal antibodies α-CN and α-CC detected CRIM1 and CRIM1-E protein in COS7 cells transfected with these constructs but not in COS7 cells transfected with pcDNA3 only (*Mock*). *C*, CRIM1-N^{myc} and CRIM1-E^{myc} protein was detected in cell lysates and conditioned media from COS7 cells transfected with these constructs by Western blotting using α-myc. A stronger band was observed in the media with transfection of CRIM1-E^{myc} than CRIM1-N^{myc}. Note the size difference observed for CRIM1 in cell lysate (140 kDa) *versus* media (120 kDa) (*arrows*). *D*, CRIM1-N^{myc} protein was detected predominantly in the light (*L*) membrane fraction of fractionated COS7 cells transfected with CRIM1-N^{myc}, with a small amount in the heavy (*H*) membrane fractions, but was not detected in the soluble (*S*) fraction. *E–H*, CRIM1 is localized on the plasma membrane with the N-terminal region in the extracellular space. CRIM1-N^{myc}-transfected COS7 cells, permeabilized with Triton X-100 (+*TX*) (*E* and *F*) or non-permeabilized (−*TX*) (*G* and *H*), were stained with either α-myc (*E* and *G*) or α-CC (*F* and *H*). The C-terminal region of CRIM1 was not detected in non-permeabilized cells (*H*). *I* and *J*, CRIM1-E does not associate with the plasma membrane. COS7 cells transfected with CRIM1-E^{myc} were either permeabilized (*I*) or not (*J*) and stained with α-myc. *K*, ideogram showing the orientation of CRIM1 at the cell-membrane. *L*, secreted CRIM1 can only be immunoprecipitated with antibodies to the N-terminal ectodomain. Cell lysates or conditioned media from CRIM1-N^{myc}-transfected COS7 cells were immunoprecipitated with α-NC or α-CC and detected by Western blotting with α-myc. Secreted CRIM1-N^{myc} is not immunoprecipitated by α-CC suggesting the loss of this epitope. *M*, CRIM1-secreted protein is glycosylated. CRIM1-E^{myc} protein treated with or without *N*-glycosidase and detected with α-myc, revealed a 10-kDa shift in molecular mass. *N*, schematic representation of potential *N*-glycosylation sites (*arrows*), as assessed by primary sequence analysis.

DESK (where *X* is presumably cysteine) was obtained after N-terminal amino acid sequencing of purified CRIM1-E, which confirms a functional signal peptide sequence with a cleavage site between amino acids Ala-34 and Leu-35.

To analyze subcellular localization we fractionated CRIM1-transfected cells to determine if it was localized to membrane fractions. CRIM1 was detected predominantly in the light membrane fraction, which corresponds to the plasma membrane compartment. A smaller concentration was evident in the heavy membrane fraction, which corresponds to intracellular trafficking compartments (Fig. 1*D*) (22). To examine potential plasma membrane localization and orientation, we analyzed CRIM1-N^{myc} transfected cells by immunofluorescence. In transfected cells that had been permeabilized by treatment with Triton X-100, there was a strong signal from antibodies to the N-terminal domain (α-myc) and the C-terminal domain (α-CC) (Fig. 1, *E* and *F*). Without permeabilization, only the N-terminal domain appeared to be accessible to antibody binding, suggesting the C-terminal was located within the cell (Fig. 1, *G* and *H*). In cells transfected with the deletion construct CRIM1-E, no cell surface localization of CRIM1-E was evident (Fig. 1*J*), yet immunofluorescence of permeabilized cells clearly showed the protein was expressed (Fig. 1*I*), suggesting that without the transmembrane domain CRIM1 is secreted. Therefore the CRIM1 protein adopts a type I transmembrane conformation with the cysteine-rich N-terminal end localized to the extracellular space (Fig. 1*K*).

CRIM1 Can Be Cleaved to Secrete a Soluble Ectodomain—Because CHRD and other CRR-containing proteins encode secreted molecules, we determined whether a secreted form of CRIM1 exists. Media harvested from COS7 cells transfected with full-length CRIM1 (CRIM1-N^{myc}) showed a small amount of CRIM1 in the media (Fig. 1*B*). The molecular mass of this form was found to be ~10–15 kDa smaller than from cellular lysates. Although CRIM1-N^{myc} from cell lysates was able to be immunoprecipitated by both α-NC and α-CC CRIM1 antibodies, only the α-NC antibody was able to immunoprecipitate the secreted form of CRIM1-N^{myc} from the conditioned media (Fig. 1*L*). These results suggest that CRIM1 is cleaved to release the N-terminal cysteine-rich ectodomain.

CRIM1 Is N-Glycosylated—Careful analysis of cell lysates and media from COS7 cells transfected with CRIM1-E^{myc} sug-

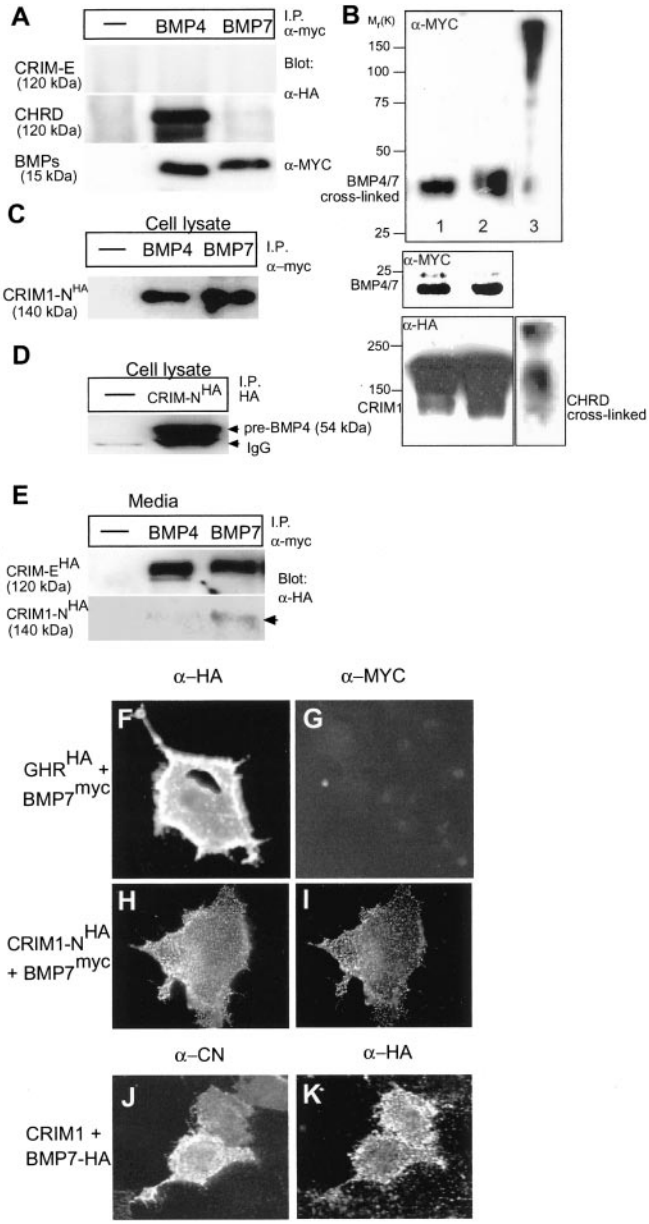

FIG. 2. **CRIM1 interacts with BMP4 and BMP7 when co-expressed.** *A* and *B*, CRIM1 does not bind to BMP4 or BMP7 when incubated in solution. *A*, co-immunoprecipitation with α-myc of CRIM1 and CHRD (5 nM) with BMP4^{myc} or BMP7^{myc} (2 nM) when incubated together *in vitro*. CRIM1-E^{HA} (*top panel*) is not co-immunoprecipitated with BMP4 or BMP7. Chordin (CHRD^{HA}) (*middle panel*) is co-immunoprecipitated with BMP4, but only weakly with BMP7. The *bottom panel* shows that the BMP^{myc} proteins were immunoprecipitated with α-myc at equivalent levels. *B*, cross-linking fails to detect an interaction between CRIM1 and BMP4 or BMP7. Conditioned media containing either CRIM1^{HA}, CHRD^{HA}, BMP4^{myc}, or BMP7^{myc} were incubated together and cross-linking performed. The media were analyzed by SDS-PAGE under reducing conditions and Western blotting using the antibodies indicated. The *top panel* shows cross-linked dimeric BMP4 (*lane 1*) and BMP7 (*lane 2*) but no evidence of either BMP4 or BMP7 cross-linked to CRIM1, which would appear as a band at ~170 kDa (BMP4 (30 kDa) plus CRIM1 (140 kDa)). BMP4 is cross-linked to CHRD (*lane 3*). The *middle* and *bottom left panels* show BMP4, BMP7, and CRIM1 prior to cross-linking. The *bottom right panel* shows the cross-linked BMP4·CHRD Western blot from *lane 3* reprobed with α HA to detect CHRD. *C* and *D*, CRIM1 can bind BMPs intracellularly when co-transfected in COS7 cells. CRIM1^{HA} is co-immunoprecipitated by BMP4^{myc} or BMP7^{myc} from cell lysates with α-myc (*C*). The precursor form of BMP4^{myc} (50 kDa) is co-immunoprecipitated by CRIM^{HA} with α-HA (*D*). *E*, CRIM1 is still bound to BMPs when secreted into conditioned media after co-transfection. CRIM1-E^{HA} (*top panel*) and CRIM1-N^{HA} (*bottom panel*) were co-immunoprecipitated with BMP4 ^{myc} and BMP7 ^{myc} from conditioned media from COS7 cells co-transfected with CRIM1-E^{HA} or CRIM1-N^{HA} and BMP4 or BMP7. *F–I*, CRIM1, but not growth hormone receptor, can tether BMPs to the cell surface. Cellular immunofluorescence with mouse α-HA (*F* and *H*) and rabbit α-myc (*G* and *I*) of non-permeabilized COS7 cells co-transfected with GHR^{HA} and BMP7^{myc} (*F* and *G*) or with CRIM1-N^{HA} and BMP7^{myc} (*H* and *I*). *J–K*, BMP7 is tethered to the cell surface as a preprotein. COS7 cells were co-transfected with BMP7^{preHA} and CRIM1-N^{HA} and cell surface proteins were detected with rabbit α-CN (*J*) and mouse α-HA (*K*).

gested a minor molecular weight disparity. To determine if this was due to *N*-linked glycosylation, we treated CRIM1-E^{myc} from media with *N*-glycosidase. This resulted in a molecular mass change of ~10 kDa suggesting that CRIM1 is *N*-glycosylated (Fig. 1*M*). Analysis of the amino acid sequence of CRIM1 suggests that there are five potential *N*-glycosylation sites (N*X*(S/T), where *X* is not P) in the extracellular domain (Fig. 1*N*).

CRIM1 and Members of the TGFβ Superfamily Can Interact—Strong evidence has suggested that CHRD-like CRR proteins bind to members of the TGFβ superfamily, particularly the BMPs (11). Due to the similarity of CRIM1 CRRs to CHRD, we have focused our analysis on BMP4 (8, 11, 12, 14). We have also investigated the possibility of interaction with BMP7, which shows overlapping sites of expression with CRIM1 in the developing kidney (19, 20). We first tested whether CRIM1 ectodomain protein harvested in media from cells transfected with CRIM1-E^{HA} or CRIM1-N^{HA} could bind mature BMPs similarly secreted into the media from BMP-transfected cells. After incubation of CRIM1 (5–10 nM) and BMP4 or BMP7 (2–10 nM) at room temperature for 1 h, there was no evidence of binding (Fig. 2*A*). Under similar binding conditions, CHRD was co-immunoprecipitated together with BMP4, and weakly with BMP7 (Fig. 2*A*), as previously described (8). To exclude the possibility that the absence of observable binding was due to a low affinity interaction between CRIM1 and BMP4, chemical cross-linking of the proteins in solution was also performed. Although the presence of cross-linked dimeric BMP4, BMP7, and BMP4·CHRD complexes analyzed under reducing conditions showed that the cross-linking was effective, no binding of CRIM1 to BMP4 was apparent (Fig. 2*B*). This suggests that the recombinant CRIM1 ectodomain does not bind BMP4 and BMP7 directly in solution. We next determined if CRIM1 could interact with BMPs intracellularly when transiently co-transfected in COS7 cells. CRIM1-N^{HA} was co-immunoprecipitated with BMP4^{myc} and BMP7^{myc} (Fig. 2*C*). In addition, the unprocessed form of BMP4 (Fig. 2*D*) was co-immunoprecipitated with CRIM1-N^{HA}. This suggests that full-length CRIM1 can bind to the precursor form of BMP4.

Because CRIM1 can be secreted into the media as an ectodomain, we determined if this form was still bound to BMPs. Both CRIM1-E^{HA} and CRIM1-N^{HA} secreted into media were able to be co-immunoprecipitated with an anti-myc antibody from conditioned media if co-expressed with BMP4^{myc} or BMP7^{myc} (Fig. 2*E*). CRIM1-N^{myc} was only weakly co-immunoprecipitated, but this may be due to the low amount of secreted CRIM1 (Fig. 1*A*). This suggests that CRIM1 can be secreted into the media as a complex with BMPs.

CRIM1 Associates with BMP7 at the Cell Surface—Because CRIM1 associates with BMPs in the cell, we used immunofluorescence analysis on non-permeabilized cells to determine if BMP7^{myc} is tethered to the cell surface when co-expressed with full-length CRIM1 (CRIM1-N^{HA}). When BMP7 is expressed alone, or co-expressed with human growth hormone receptor (GHR^{HA}), there is no BMP7-specific cell surface staining (Fig. 2, *F* and *G*). However, when BMP7 was co-expressed with full-length CRIM1, BMP7 was detected on the cell surface (Fig. 2, *H* and *I*). To determine whether CRIM1 was interacting with

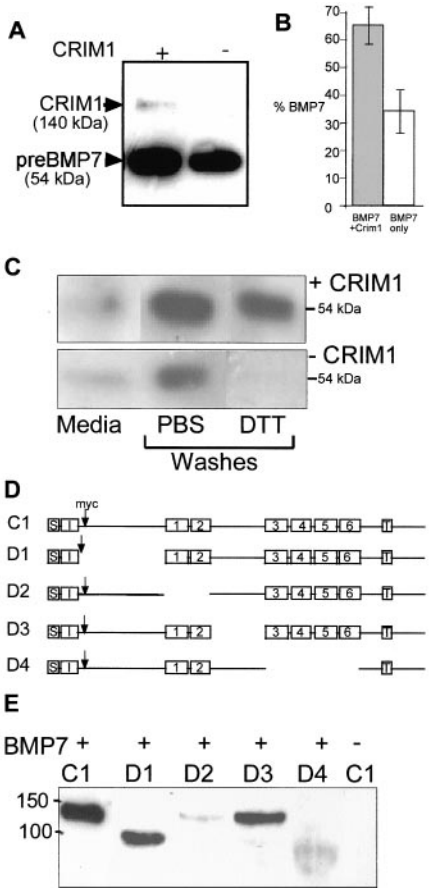

FIG. 3. **CRIM1 binds to BMPs via CRRs and retains BMP7 on the cell surface.** *A*, COS7 cells were co-transfected with CRIM1^{myc} and BMP7^{myc} or empty vector and BMP7^{myc}. Cell surface proteins were biotinylated, precipitated with streptavidin-agarose beads, and analyzed by Western blotting using α-myc. *B*, pre-BMP7 detected on the cell surface was quantitated by densitometry. The results are shown as a percentage of the total pre-BMP7 present in each experiment ± S.D. ($n = 5$). Significantly more pre-BMP7 was present on the cell surface when co-transfected with CRIM1 ($p < 0.0002$). *C*, COS7 cells were co-transfected with CRIM1^{myc} and BMP7^{myc} or empty vector and BMP7^{myc}. Live cells were subjected to a 5-min wash with PBS or 20 mM DTT, and the washes were concentrated and analyzed by Western blotting using α-myc. More pre-BMP7 was washed from CRIM1-expressing cells (*top panel*) than non-expressing cells (*bottom panel*). *D* and *E*, the CRR repeats are required for interaction with BMP7. COS7 cells were co-transfected with either CRIM1^{myc} or one of the deletion constructs (shown schematically in *D*) and BMP7^{preHA}. CRIM1 or the deletion constructs were co-immunoprecipitated with BMP7 using α HA. Immunoprecipitates were analyzed by Western blotting with α-myc. Deletion constructs lacking CRRs (D2 and D4) interact poorly with BMP7.

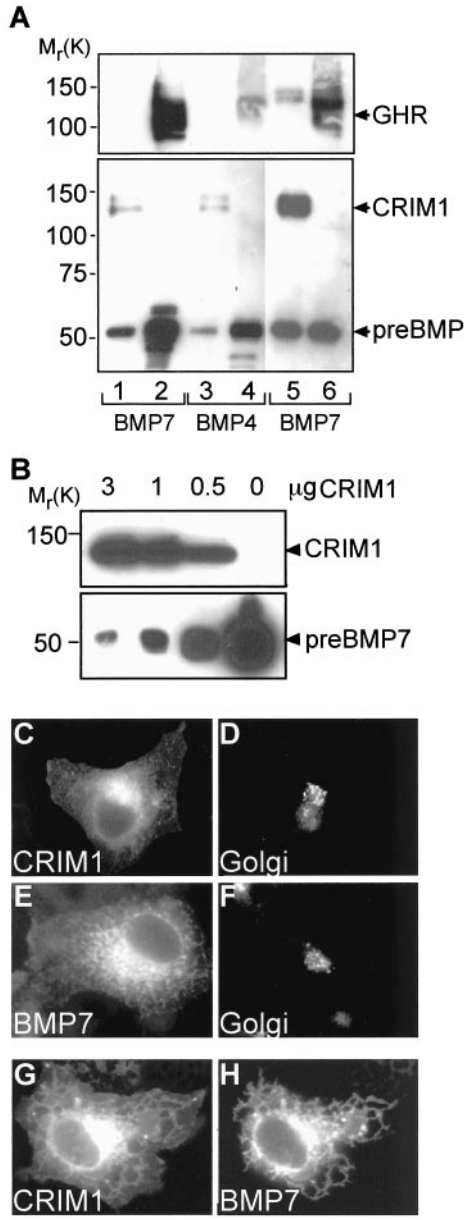

FIG. 4. **CRIM1 inhibits the co-expression of BMPs.** *A*, COS7 cells were co-transfected with CRIM1^{myc} or GHR^{HA} and BMP7^{myc} (*lanes 1* and *2*); CRIM1^{myc} or GHR^{HA} and BMP4^{myc} (*lanes 2* and *3*); D2 ^{myc} or GHR^{HA} and BMP7^{myc} (*lanes 5* and *6*). The level of expression of pre-BMP7 in cell lysates was determined by Western blotting using α-myc. To confirm expression of GHR^{HA} the blot was stripped and reprobed with α-HA. The *faint band* in *lane 5*, *top panel*, is the remains of CRIM1 binding from the initial blot. *B*, CRIM1 inhibits BMP7 expression in a dose-dependent manner. COS7 cells were co-transfected with CRIM1^{myc} (0–3 μg of vector DNA) and BMP7^{myc} (1 μg of vector DNA). Cell lysates were analyzed by Western blotting using α-myc. *C–F*, CRIM1 and BMP7 are trafficked through the Golgi. COS7 cells were transfected with either CRIM1^{myc} or BMP7^{myc}, permeabilized with Triton X-100, and co-stained with rabbit, mouse GM130 (a Golgi marker), and secondary antibodies, α-rabbit-cy3 and α-mouse-Alexa. *C* and *E* show localization of CRIM1 and BMP7, respectively, whereas *D* and *F* show localization of the Golgi in the same cells with GM130. *G* and *H*, CRIM1 and BMP7 co-localize. COS7 cells were co-transfected with CRIM1^{HA} and BMP7^{myc}, permeabilized, and co-stained with α-CN for CRIM1 (*G*) and mouse α-myc for BMP7 (*H*). The secondary antibodies used were α-rabbit-cy3 and α-mouse-Alexa. Digital images were taken on both Cy3 and Alexa channels using Image software (National Institutes of Health).

the mature or precursor form of BMP7 at the cell surface, an HA tag was introduced into the N-terminal precursor domain of the BMP7 construct. Co-immunofluorescence was performed on non-permeabilized COS7 cells co-transfected with this construct and CRIM1 using a CRIM1 antibody (α-CN) and α-HA. The results in Fig. 2 (*J* and *K*) show that the BMP7 precursor was present on the cell surface of CRIM1-expressing cells.

Biotinylation assays were used to investigate the levels of cell-surface pre-BMP7 in the presence and absence of CRIM1. COS7 cells were co-transfected with CRIM1 and BMP7 or empty vector and BMP7. Cell surface proteins were biotinylated and precipitated with streptavidin-agarose. Precipitated proteins were analyzed by Western blotting and densitometry. Fig. 3 (*A* and *B*) show that the CRIM1-producing cells retained a higher percentage of pre-BMP7 on the cell surface than non-expressing cells. To determine whether the tethered pre-BMP7 can be removed from the cell surface, COS7 cells co-transfected with CRIM1 and BMP7 or empty vector and BMP7 were subjected to a 5-min PBS wash followed by a 5-min DTT

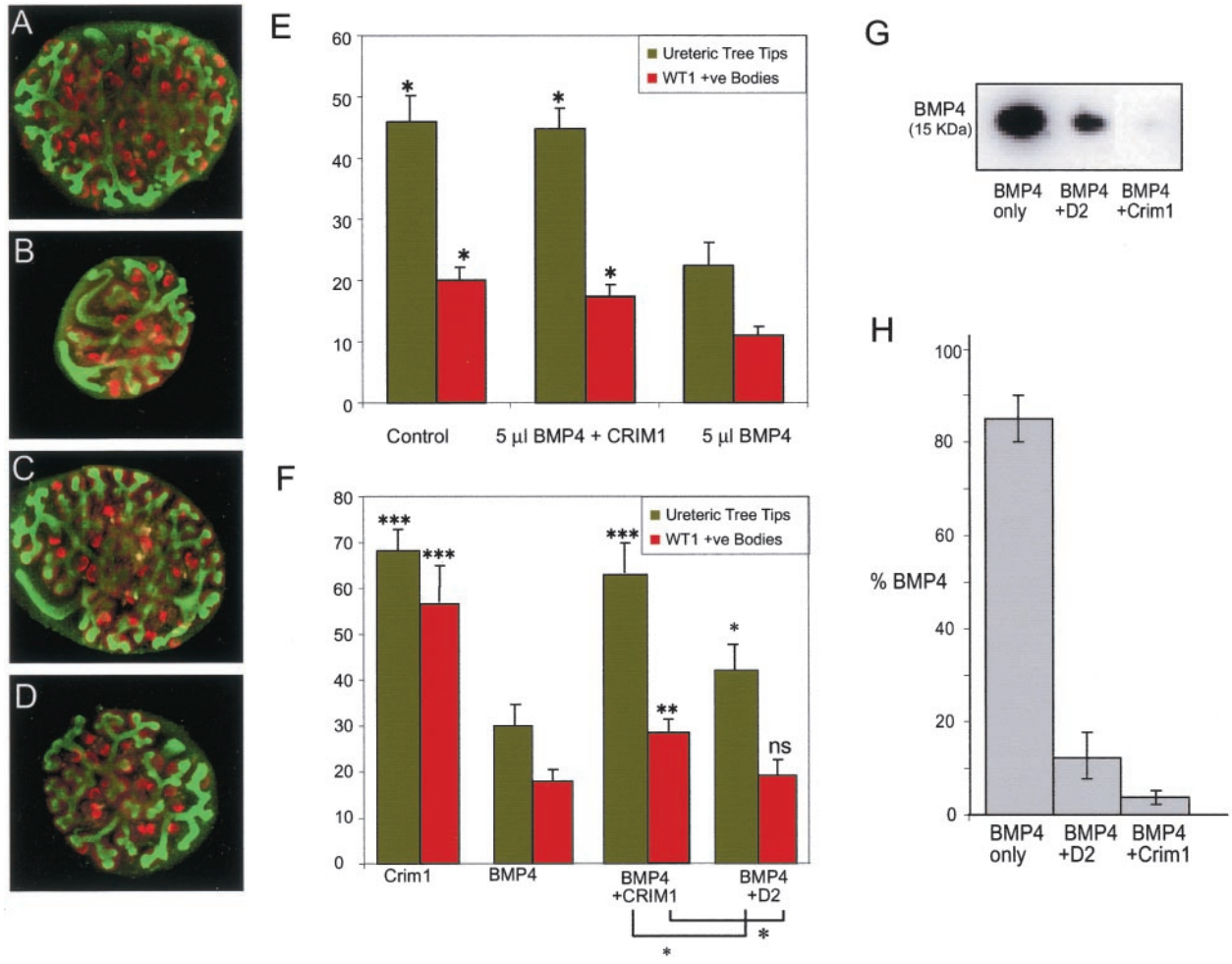

FIG. 5. **CRIM1 antagonizes the action of BMP4 by preventing secretion of mature BMP4.** COS7 cells were co-transfected with CRIM1^{myc} and BMP4^{myc} (BMP4 plus CRIM1), DelCRIM1^{myc} and BMP4^{myc} (BMP4 plus D2), BMP4 and empty vector (BMP4), or empty vector alone (control). The conditioned media from each was concentrated and added to kidney explants for 3 days as described. Immunofluorescence was performed using rabbit α-WT1 and mouse α-calbindin D-28K to detect comma and S-shaped bodies (*red*) and the developing ureteric tree (*green*), respectively (*A*, Crim1; *B*, BMP4; *C*, BMP4 plus CRIM1; *D*, BMP4 plus D2). *E* and *F*, quantitation of 12-dpc kidney explant cultures scored for WT1-positive bodies and ureteric tree tips. Experiments were performed a total three separate occasions with four to seven explants per parameter. Results are shown as mean counts ± S.D. *E*, explants grown with control and BMP4 plus CRIM1 media possess more tree tips and comma shaped bodies when compared with explants grown with BMP4 media alone (*, significant difference at $p < 0.05$). *F*, BMP4 plus D2 conditioned media resulted in a reduced number of both tips and WT1-positive bodies in comparison to CRIM1 and BMP4 plus CRIM1, but still showed a slightly higher degree of development than explants cultured with BMP4 conditioned media alone. Explants cultured with CRIM1 alone *versus* BMP4 plus CRIM1 conditioned media showed no significant difference in ureteric tree tips or WT1-positive bodies. *Asterisks within the frame* indicate significant difference between a given parameter and the same parameter when cultured with BMP4 alone. *Asterisks below the frame* indicate the degree of significance between the two conditions indicated (*ns*, not significant; *, $p < 0.05$; **, $p < 0.01$; ***, $p < 0.001$). *G*, conditioned media from these experiments was analyzed for BMP4 by Western blotting using α-myc. *H*, BMP4 in the conditioned media from BMP4 alone, BMP4 plus CRIM1 D2, and BMP4 plus CRIM1-expressing cells was quantitated by densitometry. Processed BMP4 in the media was expressed as a percentage of the total BMP4 in each experiment ± S.D. ($n = 4$). Each result was found to be significantly different at $p < 0.05$ or less. BMP4 plus CRIM1-expressing cells secreted less BMP4 than did cells expressing only BMP4. In contrast, CRIM1 D2 plus BMP4-expressing cells secreted an intermediate level of BMP4 protein.

(20 mM) wash. The washes were concentrated and analyzed for the presence of pre-BMP7 by Western blotting. Fig. 3*C* shows that a greater amount of pre-BMP7 was washed from the surface of CRIM1-producing cells, with further pre-BMP7 released from the CRIM1-producing cells after DTT treatment. These results are consistent with those of the previous experiment showing that CRIM1-producing cells retain more BMP7 on the cell surface and that the retention involves a conformation reliant on oxidized cysteine residues.

The CRR Repeats in CRIM1 Interact with BMP7—To determine whether the CRR repeats are responsible for the interaction of CRIM1 with BMPs, as in CHRD (11), a series of CRIM1 deletion constructs were made (shown schematically in Fig. 3*D*). These constructs were co-transfected with BMP7 in COS7 cells and the interaction investigated by immunoprecipitation (Fig. 3*E*). The constructs in which one of the two CRR domains were deleted (D2 and D4) interact poorly with BMP7 compared with the full-length CRIM1 and the other deletion constructs. These results suggest that the two blocks of CRR repeats, CRR1–2 and CRR3–6, bind cooperatively to ligand.

CRIM1 Inhibits Expression of BMP4 and BMP7—One unexpected observation of CRIM1-BMP co-transfections compared with BMP transfections alone was that the level of expression of the BMP4 or BMP7 was reduced when co-expressed with CRIM1. To confirm that this was a specific effect of CRIM1 expression and not an artifact due to co-expression of two constructs, COS7 cells were co-transfected with BMP7^{myc} or BMP4 ^{myc} and equimolar amounts of either CRIM1^{myc}, GHR^{HA}, or CRIM1-D2 ^{myc}. Cell lysates were analyzed by Western blotting using an α-myc antibody and then stripped and reprobed with the HA antibody to ensure co-expression of GHR^{HA}. The level of BMP7 and BMP4 expression in the lysate was

reduced markedly when co-expressed with CRIM1 but not with GHR or with CRIM1 D2 (Fig. 4*A*). COS7 cells were co-transfected with BMP7 and increasing concentrations (0.5–3 μg) of CRIM1 construct. Analysis of the conditioned media showed that secretion of BMP7 was reduced in a dose-dependent manner with increasing concentration of CRIM1 (Fig. 4*B*).

CRIM1 Co-localizes with BMP7 Intracellularly—Because CRIM1 appeared to interact with the BMPs intracellularly during processing, it would follow that the two proteins should be trafficked through the same intracellular compartments. Immunofluorescence of permeabilized COS7 cells that had been transfected with either CRIM1^{HA} or BMP7 ^{myc} showed co-localization of these proteins with GM130, a Golgi-specific antibody (Fig. 4, *C–F*). COS7 cells co-transfected with CRIM1^{HA} and BMP7^{myc} showed marked co-localization (Fig. 4, *G* and *H*).

Taken together our results suggest that CRIM1 interacts with the BMP7 precursor intracellularly, and this interaction results in decreased production of BMPs. The interaction with pre-BMPs appears to be maintained during trafficking of CRIM1 to the cell surface, where pre-BMP7 remains tethered to the cell surface.

CRIM1 Antagonizes BMP4—To examine the functional effect of CRIM1 tethering pre-BMP to the cell surface we used a kidney explant assay. BMP4 is known to retard the development of embryonic mouse kidneys grown in culture in a dose-dependent manner (23). Kidneys were dissected from embryonic mice at 11.5 or 12 dpc and were grown in culture for 3 days. Conditioned media from COS7 cells transfected with empty vector alone, BMP4 plus empty vector, BMP4 plus CRIM1, or BMP4 plus D2 were added to the cultures (Fig. 5, *A–D*). Kidneys grown in BMP4-conditioned media displayed reduced ureteric tree branching and reduced numbers of comma and S-shaped bodies compared with kidneys grown in control or CRIM1-conditioned media. BMP4 plus CRIM1-conditioned media showed a reduced BMP4 effect (Fig. 5, *E* and *F*), whereas BMP4 plus CRIM1 D2-conditioned media showed an intermediate phenotype (Fig. 5*F*). Hence CRIM1 can ameliorate the effect of BMP4. Removal of CRR1 and -2 decreases the ability of CRIM1 to act in this way. Analysis of the conditioned media by Western blotting and densitometric analysis (Fig. 5, *G* and *H*) showed that the media from the CRIM1-expressing cells contained less mature BMP4. These results support our other analyses and suggest that *in vivo* the effect of CRIM1 on BMP expression and secretion may result in a reduced concentration of active mature BMPs available to the tissues.

DISCUSSION

Proteins containing chordin-like CRRs are an important and growing family of extracellular regulators of the TGFβ superfamily. Most identified to date are secreted diffusible proteins, such as CHRD and SOG, which inhibit BMP function. Unlike CHRD and SOG, we have shown that CRIM1 is an *N*-glycosylated transmembrane protein predominantly localized to the cell membrane, but that a proportion of CRIM1 can be cleaved and released from the cell membrane as a secreted ectodomain. We also demonstrate that CRIM1 can interact intracellularly with BMP4 or BMP7, supporting the hypothesis that it will act as a mediator of TGFβ superfamily ligand activity, although not defining the specific physiological ligand. Binding of Crim1 appears to affect BMP production in three ways. There is a decrease in the production and processing of preprotein to mature BMP, the secretion of mature BMP is reduced, and a proportion of the BMP released from the cell remains associated with CRIM1, either tethered to the cell surface or as a complex in the media. These represent novel modes of BMP antagonism.

We have verified that it is the CRR repeats of CRIM1 that mediate the binding of BMPs, because CRIM1 D2 (CRRs 1 and 2 deleted) and D4 (CRRs 3–6 deleted) interact only weakly with BMP7. CHRD and other CRR-containing proteins bind to the mature, secreted form of BMP via one or more CRR. Unlike these proteins CRIM1 binds to pre-BMPs. However, because the CRR repeats of CRIM1 are necessary for binding, it is likely that interaction is still between the CRRs and the mature domain of the dimeric BMP precursor.

The intracellular interaction of CRIM1 and BMPs appears to be specific and not due to an artifact of overexpression. A nonspecific interaction between CRIM1 and BMPs within the cell would suggest the proteins were misfolded. However, the editing machinery within the cell would target the misfolded proteins for degradation within the ER (24). CRIM1 and BMP7 are clearly trafficked from the ER through the Golgi and can be secreted. Furthermore, the two CRIM1 deletion constructs D2 and D4 interact with BMP7 only weakly, whereas GHR does not interact with BMP7 at all. That BMP expression is reduced in the presence of CRIM1 also appears to be specific for CRIM1, because it does not occur with CRIM1 D2 or GHR.

The apparent role of CRIM1 in the retardation of ligand secretion is not unique. The fibroblast growth factor receptor (FGFR, also called E selectin) is localized both to the Golgi and the cell membrane. Within the cell, FGFR inhibits the secretion of its ligand, fibroblast growth factor (FGF), and maintains an intracellular pool of FGF (25). Co-expression of CRIM1 with BMPs resulted in the reduced production of BMPs. CRIM1 may inhibit processing of pre-BMPs to BMPs and thereby target the pre-BMPs for degradation or, like the FGFR, CRIM1 may sequester pre-BMPs into an intracellular pool that is limited in capacity. Once the pool is full, further expression may be inhibited. Whatever the mechanism may be, the overall effect of CRIM1 co-expression with BMPs is to reduce the amount of active mature BMPs secreted into the media, effectively resulting in antagonism.

The function of tethering of BMPs to the cell surface by Crim1 is unclear, as is the role of cleavage of the ectodomain. Tethering by CRIM1 may act to increase the effective half-life of BMPs by facilitating their slow and prolonged release from the surface, may regulate the distance over which BMPs can act, or may deliver BMPs to receptors on the cell surface. Curiously, however, our biotinylation studies suggest that it is the pre-BMP form of BMPs, which are tethered to the cell. CRIM1 cleavage does appear to occur and complexes between BMP and cleaved CRIM1 do exist in the media of co-transfected cells. This might again support the concept of delivery to receptors on another cell, restriction of the distance over which BMPs can act, or regulation of half-life in solution. Repression of secretion, tethering, and binding to the ectodomain may represent different actions tailored for different ligands. Another CRR-containing protein, connective tissue growth factor, has already been shown to bind both TGFβ1 and BMP4, delivering the former to its receptor and therefore acting as a facilitator but antagonizing the binding of the latter, thereby acting as an antagonist (18). It is possible that there are multiple roles, both positive and negative, being played by Crim1 depending upon the particular ligand bound. Further studies will be needed to clarify the versatility of Crim1 with respect to TGFβ superfamily ligand binding. However, these studies suggest that Crim1, unlike the CRR-containing proteins previously described, may function by reducing the production and secretion of active BMPs from the cells in which it is expressed. This would provide a novel level of regulation of BMP action during development and beyond.

Acknowledgments—We thank Michael Waters, Tom Jessell, Kevin Lee, and Elizabeth Robertson for expression constructs.

REFERENCES

1. Miyazono, K., Kusanagi, K., and Inoue, H. (2001) *J. Cell. Physiol.* **187,** 265–276
2. Constam, D. B., and Robertson, E. J. (1999) *J. Cell Biol.* **144,** 139–149
3. Jones, C. M., Armes, N., and Smith, J. C. (1996) *Curr. Biol.* **6,** 1468–1475
4. Dick, A., Hild, M., Bauer, H., Imai, Y., Maifeld, H., Schier, A. F., Talbot, W. S., Bouwmeester, T., and Hammerschmidt, M. (2000) *Development* **127,** 343–354
5. Sasai, Y., Lu, B., Steinbeisser, H., Geissert, D., Gont, L. K., and Derobertis, E. M. (1994) *Cell* **79,** 779–790
6. Francois, V., Solloway, M., O'Neill, J. W., Emery, J., and Bier, E. (1994) *Genes Dev.* **8,** 2602–2616
7. Schmidt, J., Francois, V., Bier, E., and Kimelman, D. (1995) *Development* **121,** 4319–4328
8. Piccolo, S., Sasai, Y., Lu, B., and De Robertis, E. M. (1996) *Cell* **86,** 589–598
9. Piccolo, S., Agius, E., Lu, B., Goodman, S., Dale, L., and De, R. E. (1997) *Cell* **91,** 407–416
10. Marques, G., Musacchio, M., Shimell, M. J., Wunnenbergstapleton, K., Cho, K., and Oconnor, M. B. (1997) *Cell* **91,** 417–426
11. Larrain, J., Bachiller, D., Lu, B., Agius, E., Piccolo, S., and De Robertis, E. M. (2000) *Development* **127,** 821–830
12. Nakayama, N., Han, C. E., Scully, S., Nishinakamura, R., He, C., Zeni, L., Yamane, H., Chang, D., Yu, D., Yokota, T., and Wen, D. (2001) *Dev. Biol.* **232,** 372–387
13. Coffinier, C., Tran, U., Larrain, J., and De Robertis, E. M. (2001) *Mech. Dev.* **100,** 119–122
14. Sakuta, H., Suzuki, R., Takahashi, H., Kato, A., Shintani, T., Iemura, S., Yamamoto, T. S., Ueno, N., and Noda, M. (2001) *Science* **293,** 111–115
15. Conley, C. A., Silburn, R., Singer, M. A., Ralston, A., Rohwer-Nutter, D., Olson, D. J., Gelbart, W., and Blair, S. S. (2000) *Development* **127,** 3947–3959
16. Matsui, M., Mizuseki, K., Nakatani, J., Nakanishi, S., and Sasai, Y. (2000) *Proc. Natl. Acad. Sci. U. S. A.* **97,** 5291–5296
17. Zhu, Y., Oganesian, A., Keene, D. R., and Sandell, L. J. (1999) *J. Cell Biol.* **144,** 1069–1080
18. Abreu, J. G., Ketpura, N. I., Reversade, B., and De Robertis, E. M. (2002) *Nat. Cell Biol.* **4,** 599–604
19. Kolle, G., Georgas, K., Holmes, G. P., Little, M. H., and Yamada, T. (2000) *Mech. Dev.* **90,** 181–193
20. Georgas, K., Bowles, J., Yamada, T., Koopman, P., and Little, M. H. (2000) *Dev. Dyn.* **219,** 582–587
21. Lovicu, F. J., Kolle, G., Yamada, T., Little, M. H., and McAvoy, J. W. (2000) *Mech. Dev.* **94,** 261–265
22. Piper, R. C., Hess, L. J., and James, D. E. (1991) *Am. J. Physiol.* **260,** C570–C580
23. Martinez, G., Mishina, Y., and Bertram, J. F. (2002) *Int. J. Dev. Biol.* **46,** 525–533
24. Ruddon, R. W., Sherman, S. A., and Bedows, E. (1996) *Protein Sci.* **5,** 1443–1452
25. Kohl, R., Antoine, M., Olwin, B. B., Dickson, C., and Kiefer, P. (2000) *J. Biol. Chem.* **275,** 15741–15748
26. Little, M. H., Wilkinson, L., Brown, D. L., Piper, M., Yamada, T., and Stow, J. L. (2001) *Am. J. Physiol.* **281,** C486–C495
27. Piper, M., Georgas, K., Yamada, T., and Little, M. (2000) *Mech. Dev.* **94,** 213–217

CRIM1 Regulates the Rate of Processing and Delivery of Bone Morphogenetic Proteins to the Cell Surface

Lorine Wilkinson, Gabriel Kolle, Daying Wen, Michael Piper, Julie Scott and Melissa Little

J. Biol. Chem. 2003, 278:34181-34188.
doi: 10.1074/jbc.M301247200 originally published online June 12, 2003
